



# Comparing surface currents near the mouth of three bays along the U.S. East Coast: Chesapeake Bay, Delaware Bay, and New York Bay

Tal Ezer<sup>1</sup> · Teresa Updyke<sup>1</sup>

Received: 22 July 2024 / Accepted: 18 December 2024 / Published online: 26 December 2024  
© The Author(s) 2024

## Abstract

Monthly surface currents at 2 km resolution near the mouths of three U.S. east coast bays were obtained from high-frequency radars (Coastal Ocean Dynamics Application Radar, CODAR) during 2012–2024. The currents near these bays, the Chesapeake Bay (CB), the Delaware Bay (DB) and the New York Bay (NB) were analyzed to infer similarity and differences, as well as potential common forcing from regional and basin-scale factors. The contribution to flow variability from local and remote forcing is evaluated by comparing surface currents with (a) river discharges into each bay, (b) with local and regional winds, and (c) with the North Atlantic Oscillation (NAO). The results show that surface flow variability near the mouth of the bays is linked with all three driving factors. The three bays often show similar flow patterns not only of the seasonal cycle, but also during extreme weather events. For example, increased surface flow into the bays from the Atlantic Ocean is seen when hurricanes are observed offshore in the fall, and increased surface flow from the bays is seen during winter storms. During positive NAO phases, eastward flow from all three bays increased due to intensified westerly winds, while during negative NAO phases flow decreased with weakening winds in the region. River discharges into the bays increased during 2012–2019 but decreased during 2019–2024. This change in river discharge trend was especially large in the CB, resulting in a change in trends of the surface currents. Monthly currents of each bay are only weakly correlated with the monthly river flow ( $R \sim 0.2\text{--}0.3$ ;  $P < 0.05$ ), while the seasonal cycles of rivers and currents have higher correlations ( $R \sim 0.6\text{--}0.7$ ). Local winds show high correlations with the monthly currents ( $R \sim 0.75$ ) with the current direction  $\sim 45^\circ$  to the right of the wind, as expected from Ekman theory. However, contributions to current variability from regional and remote factors cannot be ignored. The results demonstrate the complex nature of the currents near the mouth of bays since multiple drivers, including estuarine, coastal and open ocean dynamics contribute to the observed variability.

**Keywords** CODAR · Estuarine dynamics · NAO · Chesapeake Bay · Delaware Bay · New York Bay

## 1 Introduction

The motivation for this study comes from results of recent studies of seasonal, interannual and decadal variations in sea level, temperature, and surface currents in the Chesapeake Bay (CB, Ezer 2023a; Ezer and Updyke 2024). These studies suggest potential links between variations in this bay, which is the largest estuary of the U.S., and large-scale

variations in the Atlantic Ocean characterized for example by the North Atlantic Oscillations (NAO; Hurrell 1995) and the Atlantic Meridional Overturning Circulation (AMOC, Smeed et al. 2014; Moat et al. 2023). Since the U.S. East coast is subject to fast sea level rise and increased risk of flooding many past studies focused on sea level rise (Ezer and Corlett 2012; Ezer and Atkinson 2014; Sweet and Park 2014; Valle-Levinson et al. 2017; Domingues et al. 2018; Ezer et al. 2017; Ezer 2020b, 2022, 2023a), and potential links between offshore variations in the Atlantic Ocean and variability near the coast (Ezer 2015, 2023a; Goddard et al. 2015; Little et al. 2019; Piecuch et al. 2019; Volkov et al. 2019, 2023; Dangendorf et al. 2021, 2023; Park et al. 2022, 2024). However, not much research was done on the impact of remote Atlantic Ocean forcing on the ocean currents near

---

Responsible Editor: Joseph Zhang

---

✉ Tal Ezer  
tezer@odu.edu

<sup>1</sup> Center for Coastal Physical Oceanography, Old Dominion University, 4111 Monarch Way, Norfolk, VA 23508, USA

bays and estuaries. Unlike the existence of almost century-long tide gauge observations, current observations along the entire U.S. East coast have much shorter records, making it difficult to study decadal and longer variability.

If remote forcing is affecting variations in sea level in bays, then these variations should also affect the flow pattern and exchange between bays and the open ocean. High-frequency radar data of surface currents near the mouth of the CB indeed suggested some links with the Atlantic Ocean variability (Ezer et al. 2022; Ezer and Updyke 2024). In recent years Coastal Ocean Dynamics Application Radar (CODAR) high frequency radar (HFR) stations have been installed along long stretches of the U.S. East Coast, providing surface current data near the CB (Atkinson et al. 2009; Ezer et al. 2022; Ezer and Updyke 2024), the Delaware Bay (DB; Muscarella et al. 2011), and the New York Bay (Gopalakrishnan and Blumberg 2012; note that NB sometimes is referred to as the lower bay of New York Harbor). The existence of these new observations led us to expand the previous study (Ezer and Updyke 2024) from the CB to the DB and NB. It should be acknowledged though, that surface currents near the mouth of bays cannot fully account for the total transport in and out of estuaries, which are affected by stratification and baroclinic currents. Since there are no continuous long-term observations of the total transport in the three bays, analyzing long-term variations in surface currents near mouth of bays can provide new details on the flow that is affected by estuarine processes as well as by coastal dynamics and Atlantic Ocean variability. Classic estuarine circulation is well described in the literature as driven by freshwater river discharge at one end and saltwater intrusion and tidal mixing at the other open end, though circulation can be quite complex and vary from bay to bay due to topography, stratification, and other factors (Valle-Levinson et al. 1998, 2003; Valle-Levinson 2010). Short-term observations near the mouth of bays show that subtidal current variability is mostly driven by the local winds, as shown for example near the mouth of the DB (Wong and Garvine 1984; Garvine 1991; Muscarella et al. 2011). However, Garvine (1991) noted that near the mouth of the bay along-coast local winds drive short-term current fluctuations, while river flow into the bay only affects currents there on time scales of weeks and longer. In fact, not many studies address long-term variabilities in bays beyond the tidal and seasonal time scales, which motivated us to look at relatively long records beyond the tidal-dominated daily flow. By comparing three different bays, separated by ~400 km, having different topographies and different river inputs, we try to evaluate what part of the dynamics is locally driven versus potential common forcing from large-scale climate patterns. The study may have important implications for coastal ocean prediction, since remote forcing from the open ocean on the coast is not well understood or predicted.

The study is organized as follows. First, the data sources and analysis methods are described in Sect. 2, then results are presented in Sect. 3, focusing on correlations between the bays, river discharges, winds and Atlantic Ocean variability. Finally, summary and conclusions are offered in Sect. 4.

## 2 Data sources and analysis methods

Monthly surface currents were obtained from High Frequency Radar (HFR) data archived at <https://cordc.ucsd.edu/projects/hfrnet/>; data on the 2 km grid from March 2012 to March 2024 were extracted for the U.S. East Coast from the Scripps Institution of Oceanography National HFR Network data catalog (HFRNet; <https://hfrnet-tds.ucsd.edu/thredds/catalog.html>). Note that monthly statistics are only computed for locations with at least 70% data availability. The data were further extracted for three subregions near the mouth of the three bays of this study (Fig. 1). The data represent flow in the upper meter of the water column. Most of the study focused on analysis of zonal flow (U-components of surface currents), where positive values represent general flow from the bay toward the Atlantic Ocean. This allows us to compare the three bays with the same zonal wind, which dominates the region. It is noted that the previous study that focused only on the CB (Ezer and Updyke 2024) used our locally maintained HFR observations (<http://www.ccpo.edu/currentmapping/>; see also Atkinson et al. 2009 and Ezer et al. 2022) with slightly different quality control, a different period (2007–2021) and a focus on flow toward the south-east. However, comparison between the local institutional data and the public (HFRNet) data used here shows that the two data sets are generally consistent with each other during the overlapping period of the two studies, and differences in trends are due to the period used (more on this later). The chosen area near the mouth of the bays was based on the availability of the 2 km high resolution observations. Moreover, since the analysis is focused on area mean and monthly mean time series, slight changes in the chosen area did not make any significant difference in the results.

Monthly river streamflow into the CB, which includes several rivers and streams, was obtained from: <https://exchange.iseesystems.com/public/samuel-austin/chesapeake-bay-estimated-streamflow-test-model/index.html#page1>. Monthly river discharges into DB and NB were obtained from USGS (<https://waterdata.usgs.gov/nwis/monthly/>) – using Delaware River data (USGS station 01463500), and Hudson River data (USGS station 01358000), respectively. Variations in the Delaware River flow dominate the circulation and water properties of the DB (Sharp et al. 1986), and the Hudson River provides most of the discharge water into NB (Li et al. 2019), so that unlike the CB, a single river

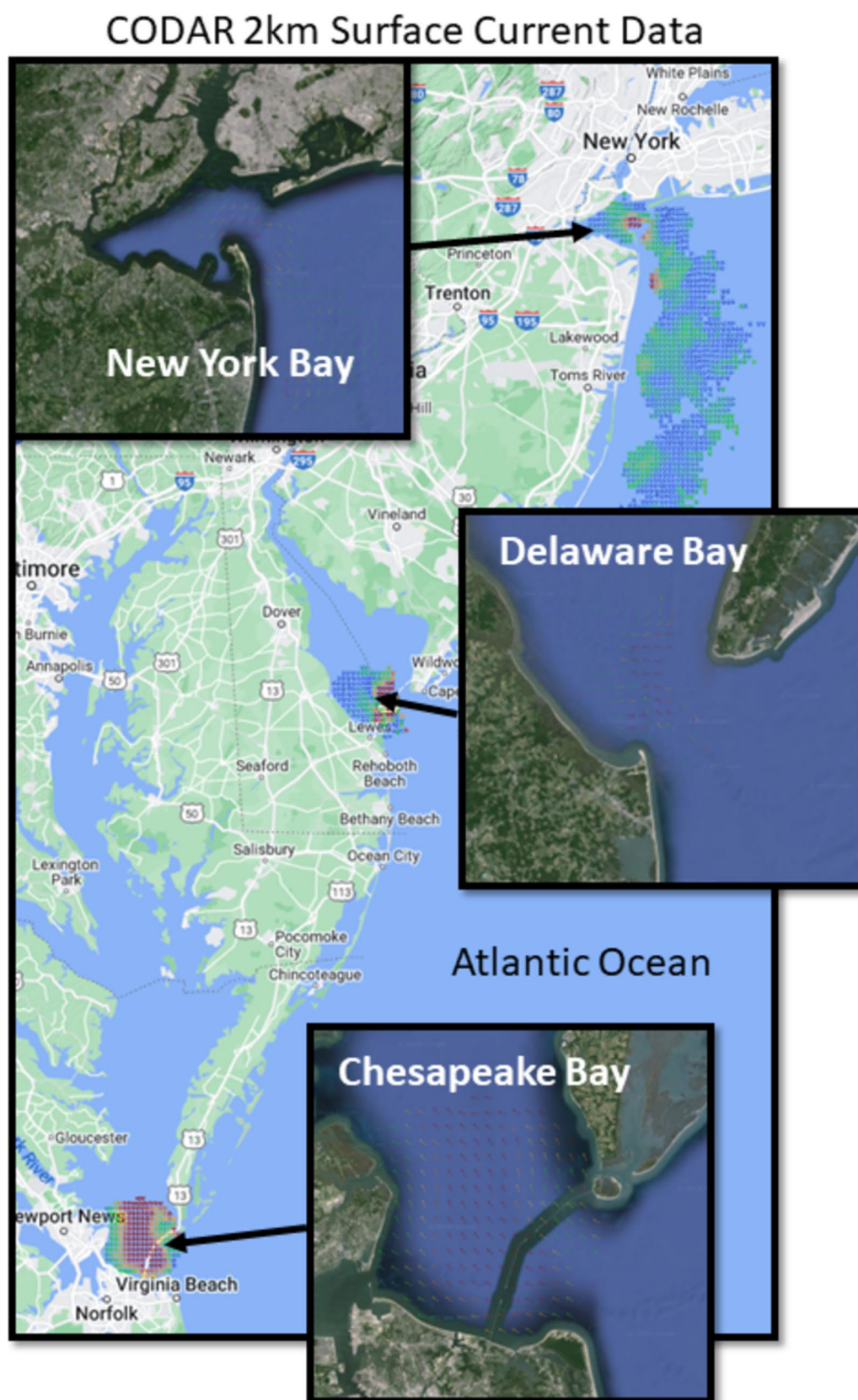


**Fig. 1** A map of the study area and the CODAR 2 km data for the three locations: Chesapeake Bay (CB), Delaware Bay (DB) and New York Bay (NB). The surface currents shown here are examples during arbitrary day, for mean currents over the study period see Fig. 2



discharge is sufficient for these two bays. The streamflow units were converted from  $\text{ft}^3\text{s}^{-1}$  as reported by USGS to  $\text{m}^3\text{s}^{-1}$ . Also, because the flow into the CB is much larger than that of the other two bays, in some analysis, streamflow into the CB was divided by a factor of 4 to allow plotting on the same axis.

Monthly North Atlantic Oscillation (NAO; Hurrell 1995) Index was obtained from NOAA's Climate Prediction Center (<https://www.cpc.ncep.noaa.gov/products/precip/CWlink/pna/nao.shtml>). NAO is related to wind patterns over the Atlantic Ocean that may affect currents along the U.S. East Coast, so wind pattern data from NCEP/NCAR Reanalysis were obtained from NOAA's Physical Science Laboratory (<https://psl.noaa.gov/data/reanalysis/reanalysis.shtml>). Local wind data were obtained from NOAA stations (<https://tidesandcurrents.noaa.gov/>); monthly means were calculated from the original 6-minute data.

Statistical analyses of these data include calculating correlation coefficients between time series of the same type of data, e.g., transport in river#1 versus river#2, as well as correlations across different sources, e.g., transport of river#1 versus flow in bay#1. Cross correlations were also calculated to see if lags exist between time series. Linear trends of each time series were also calculated, but one should keep in mind that 12-year records are too short for assessing long-term climatic trends and decadal variability. As shown later, a large anomaly in one or two years can significantly change the trend during this relatively short period.

### 3 Results

#### 3.1 Surface currents in the three bays: pattern, trend, and impact of extreme events

The mean surface current pattern over the study period (March 2012 to March 2024) shows some similarity and some differences between the three bays (Fig. 2). In all three bays, the strongest flow is seen in the southern side of the mouth of the bay - this pattern can be partly explained by the right turn of the bay of the freshwater plume due to Coriolis (Galperin and Mellor 1990; Garvine 1991). In addition, topography could enhance wind-driven flow pattern where the currents are directed toward the deep channel and exit the bay at the deepest part of the mouth (this is seen most clearly in the DB and CB). The DB has a distinctly different pattern than the other two bays with a strong southwestward flow in the lower bay - this may be due to the topography of the lower DB which has deeper and wider channel than the other bays. The pattern of the mean surface currents in DB is indeed like in previous observations (Wong and Garvine 1984; Garvine 1991; Muscarella et al. 2011) and in models (Galperin and Mellor 1990). The mean surface currents shown in Fig. 2

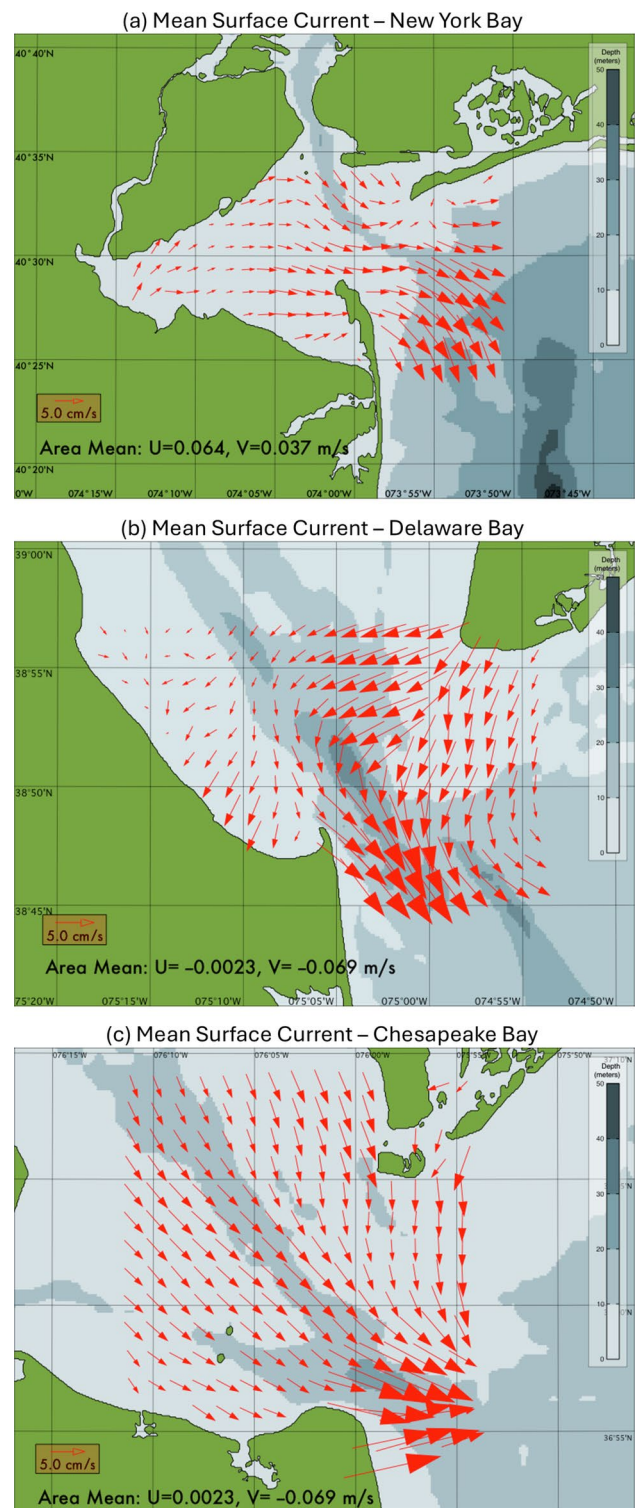


**Fig. 2** Mean surface currents over the period March 2012–March 2024 near the mouth of the three bays. Bottom topography and depth are indicated by the gray background

are also like those in past studies of the CB (Atkinson et al. 2009; Ezer et al. 2022; Ezer and Updyke 2024) and the NB (Blumberg et al. 1999; Gopalakrishnan and Blumberg 2012; Li et al. 2019). However, while most of these past studies focused on short-term tidal and wind-driven variability, here interannual and longer time scales are analyzed, as well as remote influence from the Atlantic Ocean.

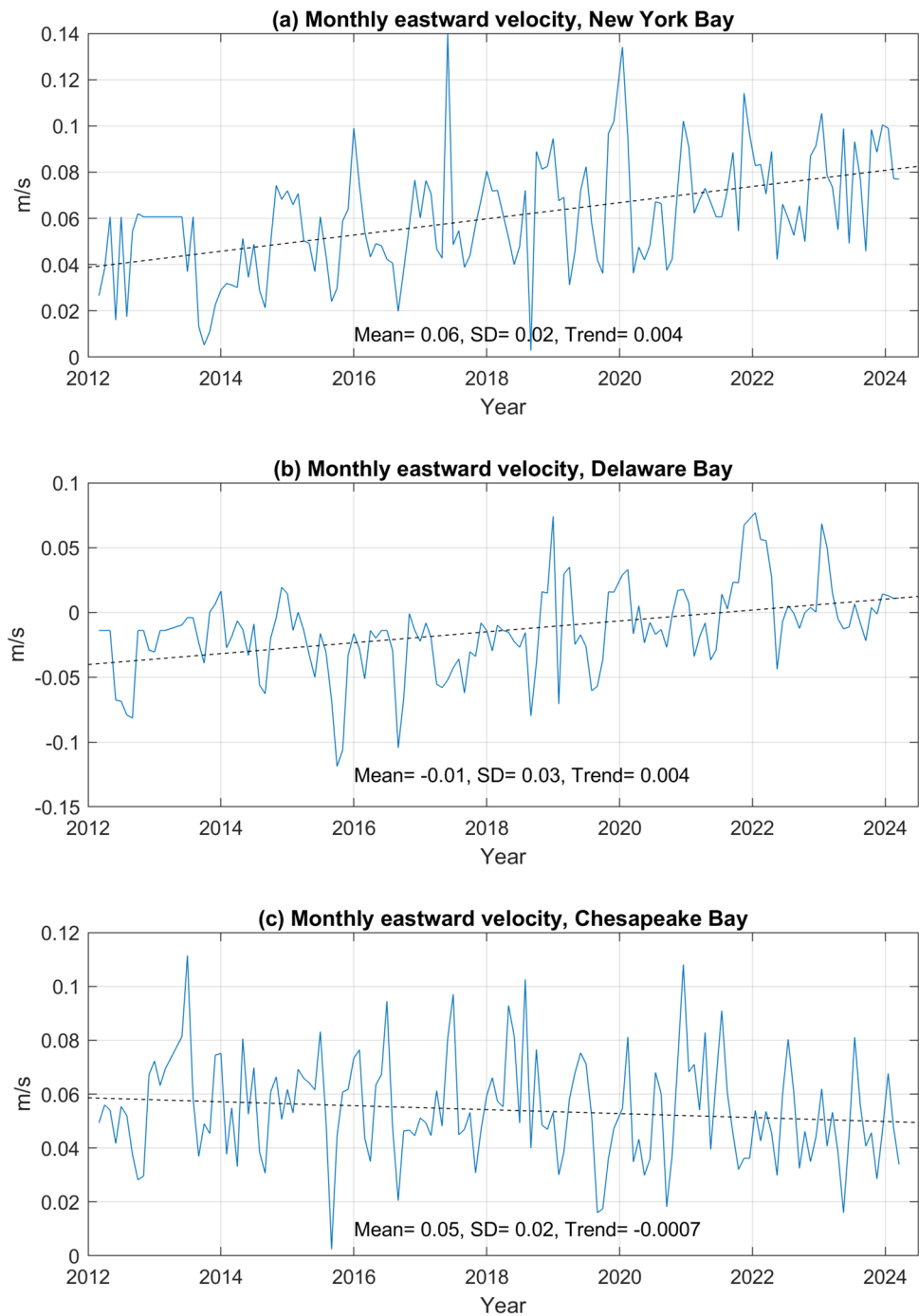
Since each bay has a slightly different flow pattern near its mouth, we analyzed the zonal component (surface eastward U-velocity, hereafter referred to simply as “velocity” or “flow”) averaged over the regions in Fig. 2. This analysis is meant to generally represent flow from the coast toward the Atlantic Ocean. Note that Ezer and Updyke (2024) rotated the vectors toward the southeast, but trends and variability seem very similar to the U-velocity since the flow direction near the mouth of CB changes very little in this region (Fig. 2c). Using the same eastward flow in all three bays (rather than having different rotation in each bay) allows a more meaningful comparison with zonal wind. The chosen area extends beyond the mouth of the bay because there is too much missing data in the mouth itself. The monthly time series of the flow are shown in Fig. 3. The upward trend of increased flow from NB and DB of about 4 cm/s per decade (Fig. 3a and b) is consistent with the increased precipitation and river discharge in the northeastern U.S. (Rice et al. 2017). However, the insignificant trend in the CB outflow of  $-0.7$  cm/s per decade (Fig. 3c) in 2012–2024 seems to be different than the results of Ezer and Updyke (2024) who found in CB increased flow of 2.2 cm/s per decade in the earlier period of 2007–2021. During the overlapping period the two studies generally agree with each other, despite differences in the source of data and the area used for averaging. The results from both studies show increased flow from CB of 3.3 cm/s per decade from 2006 to 2016, but only 0.3 cm/s per decade from 2016 to 2021 and further reduced from 2021 to 2024 as seen in Fig. 3c. The reason for the change in flow trend over time (change in river discharge) will be discussed later in detail. It is also not unexpected that decadal variability such as those associated with the North Atlantic Oscillation (NAO; Hurrell 1995) and the Atlantic Meridional Overturning Circulation (AMOC; Moat et al. 2023) can affect the bays, as suggested by Ezer and Updyke (2024), but longer observations than the 12-year data used here, are likely needed to capture these decadal variations.

To assess if there is a large-scale common driver for the three bays, correlations between the flow from the bays are calculated after removing the trends (Fig. 4). The results indeed show statistically significant correlation coefficients (Table 1), whereas the highest correlation is found between the two northernmost bays, DB and NB (99.999% confidence level), and the lowest correlation (99% confidence level) was found between the two southernmost bays, CB and DB. The multiple rivers and the large

watershed of the CB probably makes its variability more complex than if driven by a single major river like DB and NB. While having statistically significant correlation coefficient ( $R$ ) demonstrates relations, it does not indicate the cause of the relation. It is also noted that even the larger correlation coefficient between NB and DB ( $R = 0.41$ ) means that only about 17% of the variability ( $R^2 = 0.17$ ) is explained by this common driver, while other factors contribute the rest of the variability, as seen later.

Figure 5 shows the monthly flow anomaly (detrended time series) of the three bays, indicating several unusual peaks where all the bays have similar anomalies. Negative anomalies that indicate increased flow into the bay were identified at periods when hurricanes were observed off-shore of the U.S. East Coast. Studies of these hurricanes show increased coastal sea level, due to storm surge and weakening of the Gulf Stream by the storms (sometimes for weeks after the storm). Therefore, when storms move along the U.S. East Coast, they cause additional transport of water toward the shore and into the bays, and this is consistent with the increased flow toward the bays as seen in the negative peaks in Fig. 5. The impact of storms on bays largely depends on the track of the storm and its intensity, so here we show only a few examples. More information on the hurricanes indicated in Fig. 5 can be found in recent studies of Hurricane Joaquin in 2015 (Ezer and Atkinson 2017), Hurricane Matthew in 2016 (Ezer et al. 2017; Park et al. 2022, 2024), Hurricane Florence in 2018 (Ezer 2019) and Hurricane Dorian in 2019 (Ezer 2020b). Note that tropical storms and hurricanes occur mostly during the fall, when the seasonal sea level is higher with the so-called “King Tide” (Ezer 2020a). On the other hand, positive peaks in Fig. 5, which represent larger than normal flow out of the bays, occur recently (since 2018) mostly in the winter around January. These anomalies may be related to the increase in extreme snow events over the U.S. due to global warming (Chen et al. 2021). Close examination of the period of these peaks found that they are indeed associated with winter storms that passed over the northeastern U.S. For example, the largest peak in outflow in the DB occurred in January 2019, during the “Harper” winter snowstorm event in middle January 2019 ([https://www.weather.gov/pah/SnowJan19\\_2019](https://www.weather.gov/pah/SnowJan19_2019)). During this period a weak jet stream and an extreme cold wave (called a “Polar Vortex” by the media) were seen. Winter storms named “Jacob” and “Isaiah” in January 2020 coincide with peak flow in all three bays seen in Fig. 5. Another big winter storm occurred in January 2022 (<https://www.weather.gov/akq/Jan22-2022Snow>), which again coincides with peak flows. Storms occur over short time scales of days, and have much larger impact on daily radar data, but they seem to have enough impact to influence the monthly data analyzed here.

**Fig. 3** Monthly zonal surface velocity (U-component) averaged over each region of Fig. 2. The mean, standard deviation, and trend (in m/s per year) are indicated, as well as the linear trend line

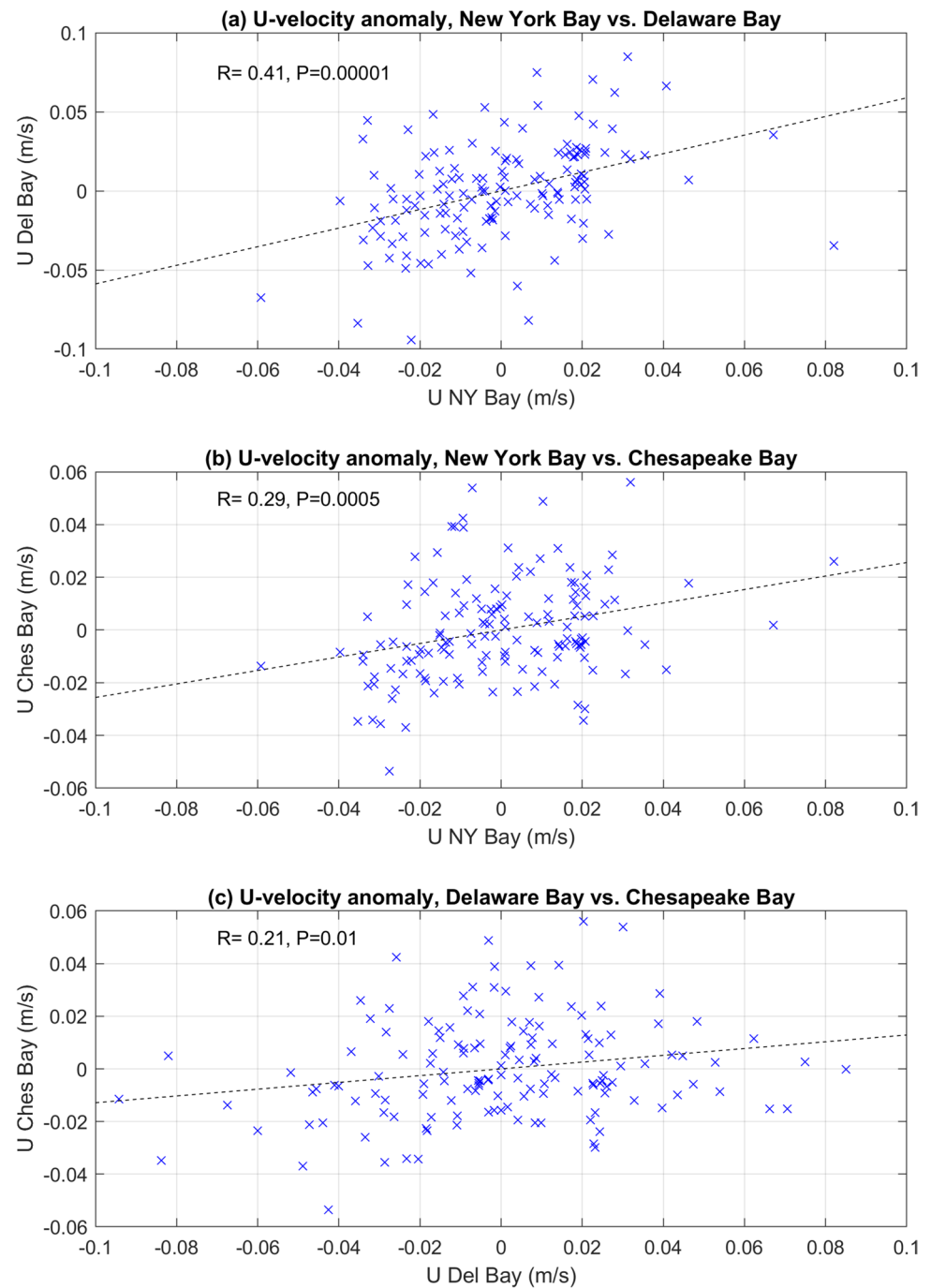


### 3.2 Comparison of surface currents with river discharge

Classical estuarine circulation is usually described as driven by freshwater discharge from rivers at one end and tides from the open ocean on the other end (Valle-Levinson 2010), so when analyzing monthly data, which removes the daily tides, river discharge should have strong influence on the seasonal and interannual variability of flow from bays. Figure 6a shows the monthly river inflows into the bays;

these river discharges are highly correlated with each other ( $R=0.64\text{--}0.85$ ; Table 1). While seasonal variations are dominating the variability, large interannual variations are also seen. Especially large discharge is seen around January 2019, during the winter snowstorm and the extreme cold wave of the northeastern U.S. as discussed before in Sect. 3.1. The result is a change of trend (dash lines in Fig. 6a) whereas river discharge increased before 2019 and decreased after 2019. The smallest change in trend is in the Hudson River (from +15 to -25 m<sup>3</sup>/s/yr) and the largest change in CB

**Fig. 4** Scatter plots and correlations between the detrended flows of the three bays. Statistical significance of the correlation coefficients range between 99% (DB vs. CB; Fig. 4c) and 99.999% (DB vs. NB)



streamflow (from +234 to −298 m<sup>3</sup>/s/yr). The differences in river flow are even more dramatic after applying a 24-month Hanning Filter (Fig. 6b), indicating unusually large stream flow into the CB during 2018–2019 (and to lesser degree in DB). This anomaly in river flows into the CB, results in a change in eastward currents trend from positive before 2019 to negative after 2019 and explains the apparent discrepancy between the result shown here of a negligible flow trend for 2012–2024, and the results of Ezer and Updyke (2024) of upward trend in earlier years.

Figure 7 shows comparisons between flow velocities and river discharges in the bays (left panels of Fig. 7); correlation coefficients are not very large, but all are statistically significant at over 95% confidence level (Table 1). The cross correlations between river and current flows (right panels of Fig. 7) show clear seasonal cycle (12-month lags between peaks) but somewhat asymmetric cross correlations pointing to contribution from interannual variability. The lower correlation of CB at zero lag relative to the other bays may indicate that this bay may have larger contribution to its



**Table 1** Correlation coefficients between variables for March 2012 to March 2024 (except local wind in NB that started May 2015). U is the zonal surface velocity anomaly (detrended) near the mouth of the 3 bays (CB, DB, NB) and R is the monthly river discharge into each bay (maximum correlation of the seasonal cycle with lag is also indicated). Reginal wind is the near surface U-component from reanalysis (2.5 x 2.5 grid point centered near the three bays) and local

wind is for the maximum correlation with NOAA local wind stations near each bay when considering Ekman veering to the right of the wind (Fig. 10). The comparison with NAO is after a 6-month Hanning Filter. Background colors represent correlations between different variables. Only correlations with statistical significance over 95% ( $P < 0.05$ ) are shown

currents			rivers			wind		NAO	
U-CB	U-DB	U-NB	R-CB	R-DB	R-NB	regional	local		
-	0.21	0.29	0.20 (0.4)	←monthly ←seasonal		0.25	0.74	0.21	U-CB
	-	0.41		0.27 (0.7)		0.55	0.61	0.28	U-DB
		-			0.26 (0.6)	0.61	0.76	0.26	U-NB
			-	0.85	0.64				R-CB
				-	0.73				R-DB
					-				R-NB

**Fig. 5** Monthly time series of the anomaly flow (detrended) in CB (red line), DB (green line) and NB (blue line). Several peaks where similar anomaly is seen in multiple locations are indicated. Negative peaks (larger than normal surface flow into the bay) associated with offshore hurricanes are seen in the fall (September–October; see inset boxes), while positive peaks (larger than normal flow out of the bay) associated with winter storms are seen recently in January

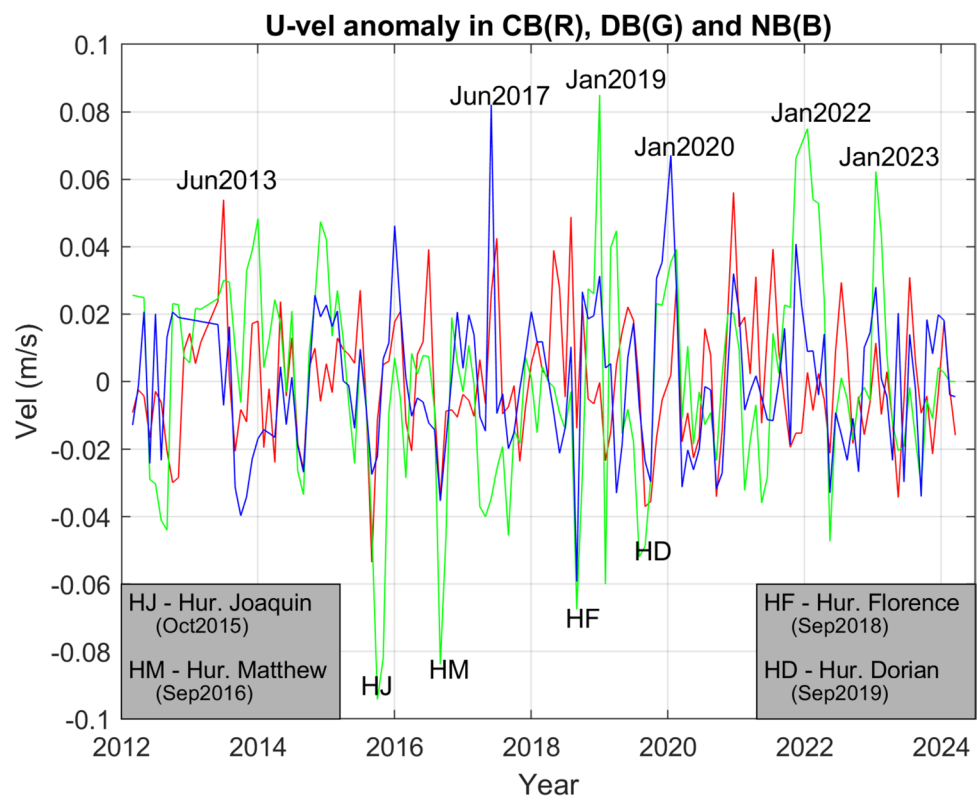
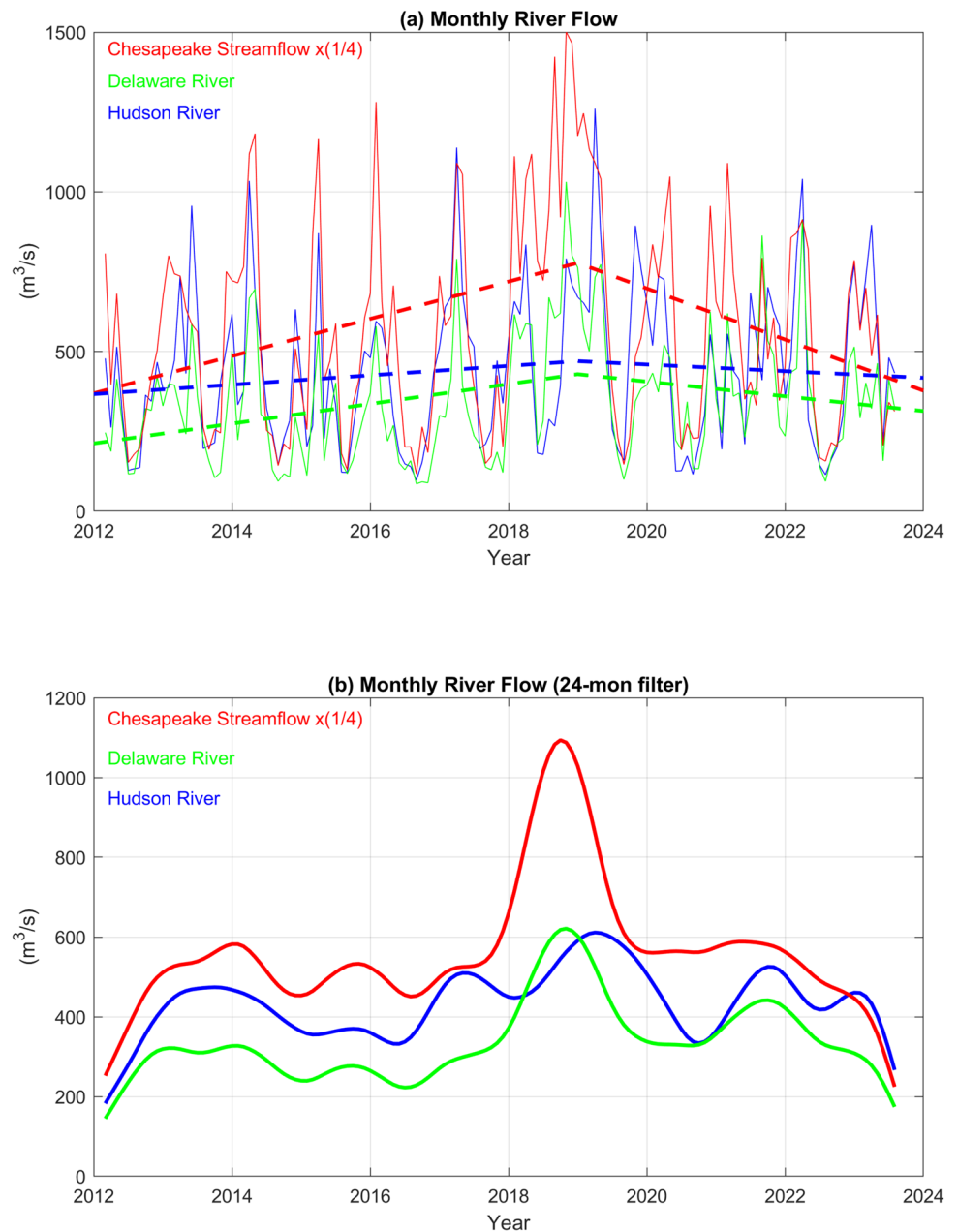




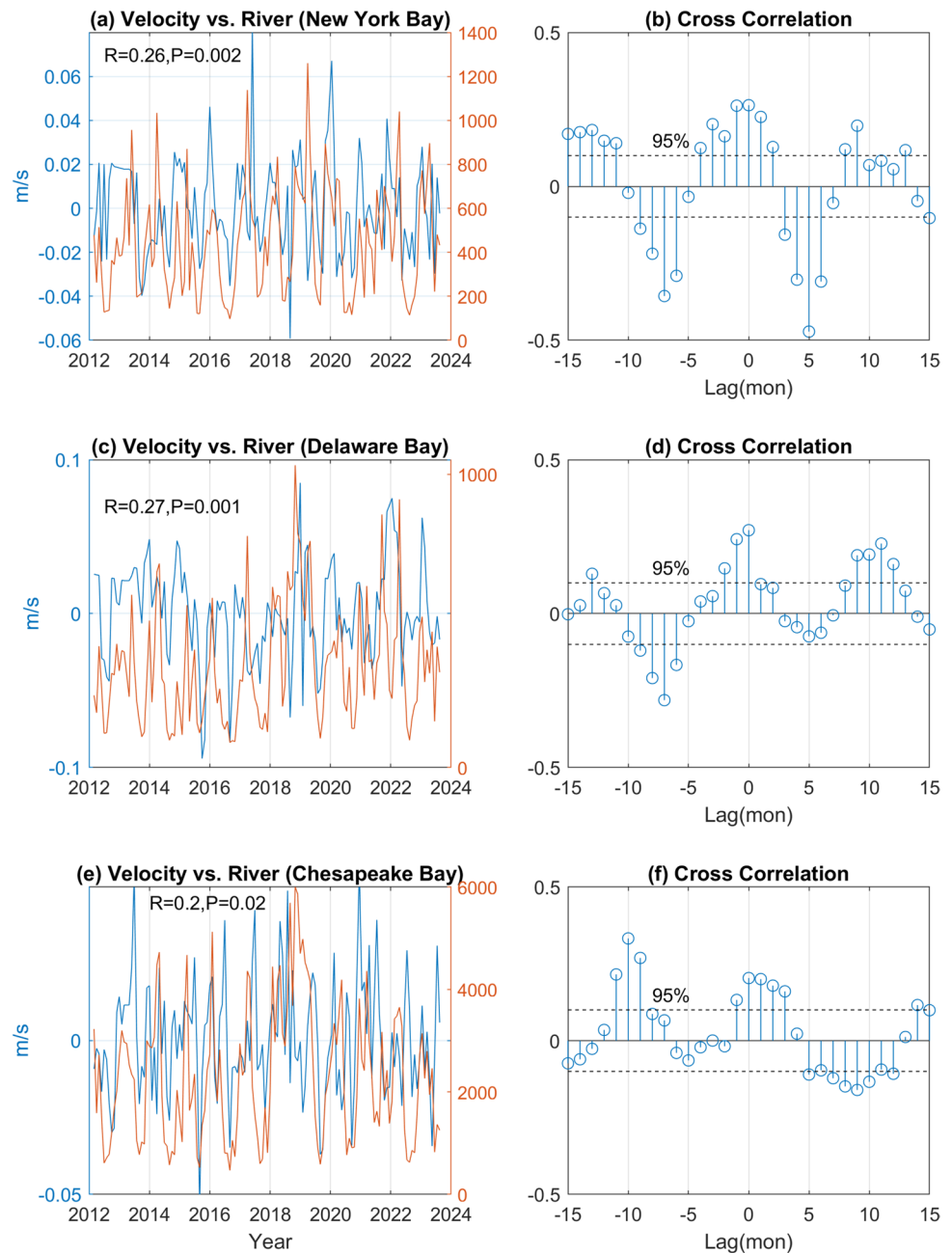
**Fig. 6** Transport of rivers and streams into the bays: sum of streamflow into CB (red line; value divided by 4), Delaware River discharge into DB (green line) and Hudson River discharge into NB (blue line). **a** Monthly data. **b** After applying a 24-month Hanning Filter. Trends in **a** are shown (dash lines) before and after 2019. The trends (in  $\text{m}^3/\text{s}$  per year, [before, after]) are: CB [234, -298], DB [31, -25], NB [15, -25]



flow variability from sources other than rivers. Looking closer at the seasonal cycle from monthly averages over the entire period shows maximum spring river flow occurs around April (Fig. 8a) while maximum westward surface velocity occurs in July in the CB, but in January in DB and NB (Fig. 8b). All three bays show minimum velocity in September (negative anomaly indicates more westward flow, i.e., weaker outflow from the bays), when river discharges are also very weak. The standard deviation from the monthly mean (error bars in Fig. 8) indicates that river flow has much more pronounced seasonal cycle than the velocity does, again indicated that the flow is affected by factors other than rivers. When comparing the seasonal cycle of velocity

to that of sea level (Ezer 2020a, 2023a) it is found that maximum sea level occurs in the fall when flow increases from its minimum. Cross correlations between the seasonal pattern of river discharges and surface flows shows somewhat different pattern for each bay (Fig. 9), as also can be seen in Fig. 8. Only the CB shows significant lag of 2–3 months between the river and velocity flows (as seen in Fig. 8, maximum river discharge into CB occurs in April–May and the maximum outflow is in July). Only DB shows statistically significant correlation of the seasonal cycles at zero lag. The maximum correlation coefficient (including lag) indicates that the seasonal cycle of rivers is responsible for about 40% of the variability of the seasonal velocity cycle ( $R^2 \sim 0.4$ ).

**Fig. 7** Left panels: monthly eastward velocity (m/s, blue, y-axis on the left) and river discharge (m<sup>3</sup>/s, red, y-axis on the right). Right panels: Cross correlations; dash lines represent estimated 95% confidence level for the correlation coefficients

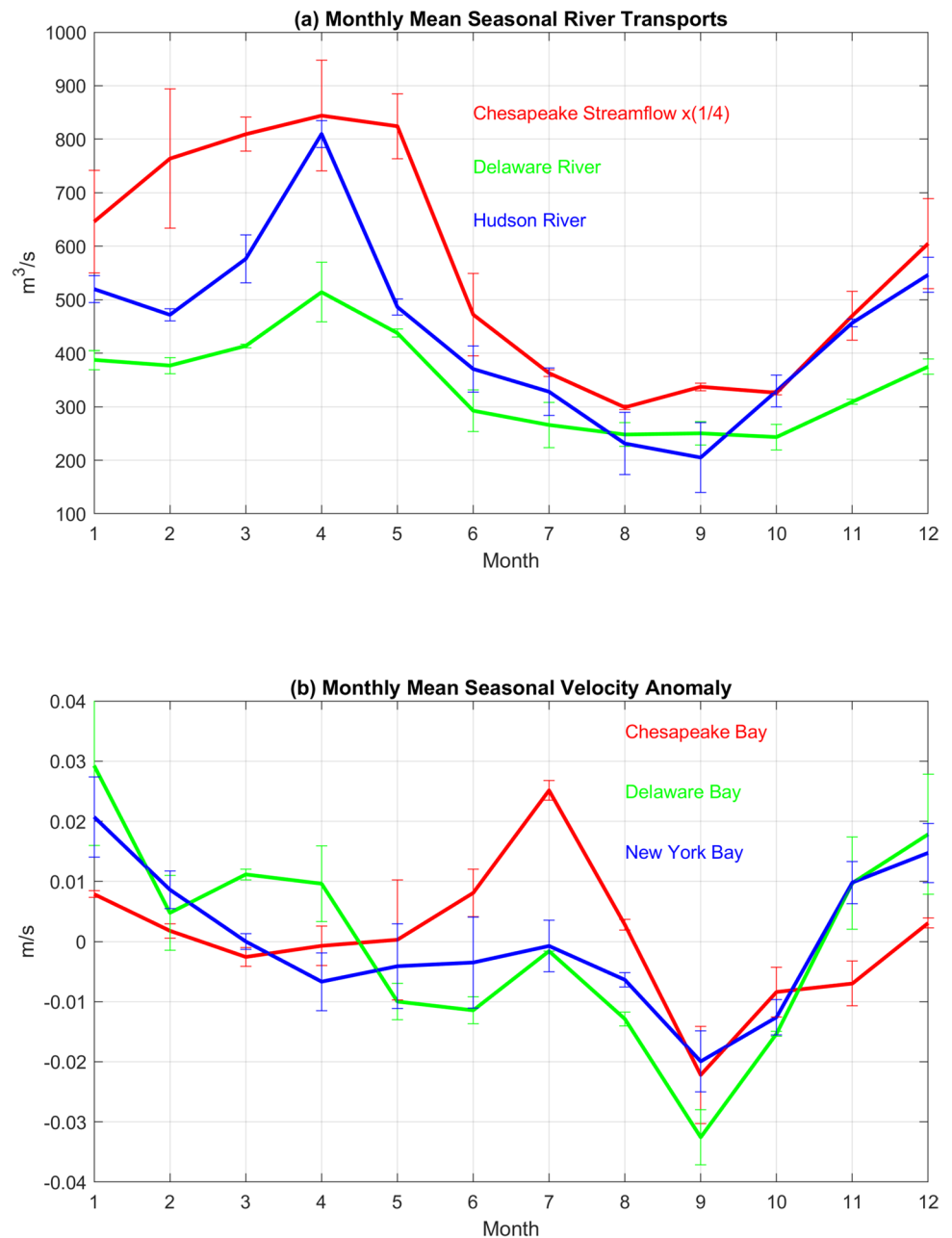


### 3.3 Comparison of currents with winds and NAO

As demonstrated in the previous section, flows near the mouth of the bays are correlated with river discharges, as expected, but the correlations indicate that river discharge is only responsible for some part of the monthly flow variability. Other potential sources of variability include local winds and large-scale atmospheric and oceanic variations over the Atlantic Ocean. Daily variations in upper ocean currents are generally driven by surface winds, for example by the Ekman flow (e.g., see recent evaluation of the Ekman Theory by Ezer 2023b). Wong and Garvine (1984) for example,

indicated that the coastal flow variability near the mouth of DB is driven by along coast wind-driven Ekman transport. Short-term observations by Muscarella et al. (2011) indeed show that subtidal surface currents near the mouth of DB were mostly driven by local wind and affected by local topography and coastal dynamics, explaining the spatial pattern seen in DB here (Fig. 2b). Figure 10 shows the correlation between local monthly wind at 4 stations near the mouth of CB and the eastward current anomaly (east and north components of the currents and the winds were used to calculate the angle between the wind and current, but only correlation of the eastward flow is shown). At Cape

**Fig. 8** Seasonal cycle of **a** river discharges and **b** eastward velocity anomaly. Error bars on each monthly mean represent one standard deviation. Note that in **a**, the river discharged into CB is divided by 4 so the discharge into all bays can be shown on the same axis



Henry, the location closest to the mouth of CB, the highest correlation ( $R=0.74$ ) is found when the current is  $45^\circ$  to the right of the wind, as expected from the Ekman theory in the northern hemisphere. At two other stations (CBBT and Willoughby) the angle of maximum correlation is about  $30^\circ$ , while at one station, farther north of the currents (Kiptopeke), the angle of maximum correlation is about  $20^\circ$ . These results indicate some spatial variations in the wind pattern, which is not unexpected. Local wind observations near the other two bays are scarce with only one or two stations that include some gaps- they show maximum local wind-current correlations of  $\sim 0.6$  in DB and  $\sim 0.75$  in NB (Table 1). All these correlations have significant level of over 99.99%, but

also indicate that about 50% of the monthly current variability is contributed by factors other than local winds.

The results here are consistent with past observations such as Wong and Garvine (1984) that show short-term coastal wind-driven Ekman flows near the mouth of DB. However, what about current variability related to long-term and large-scale wind patterns? In Fig. 11 the eastward current velocities in the three bays are compared with the mean zonal wind (U-component) obtained from reanalysis over the entire region (the V-component of the wind is extremely small in the reanalysis over this region). The wind data is area mean of  $2.5^\circ \times 2.5^\circ$  box centered at  $75^\circ\text{W}$ ,  $40^\circ\text{N}$ , thus representing the large-scale wind pattern over the western

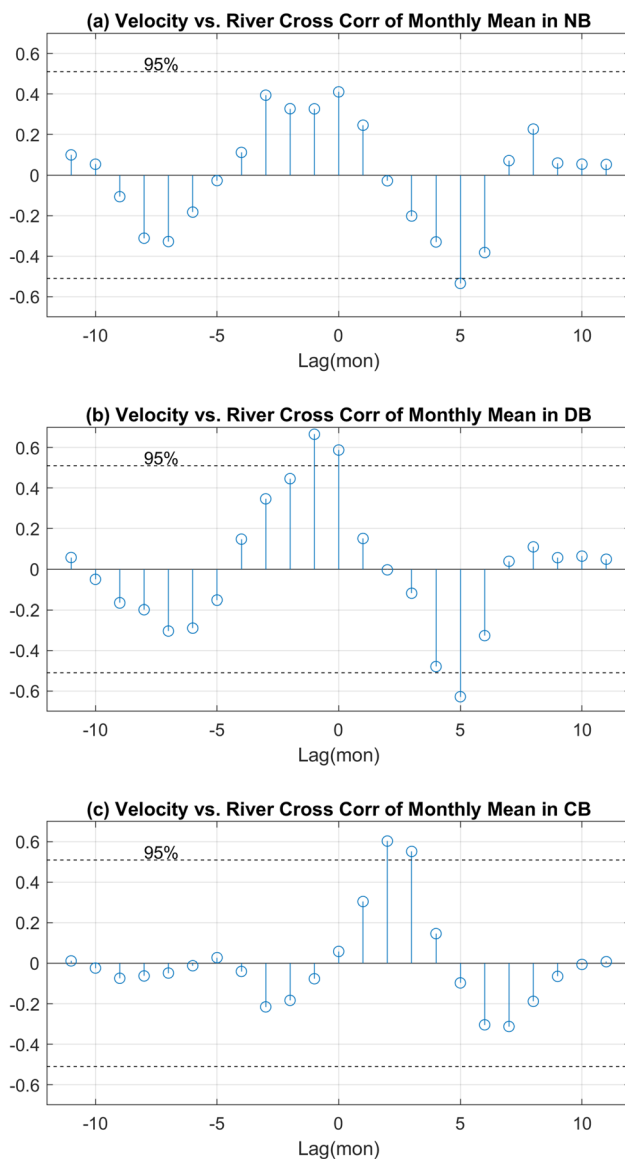


**Fig. 9** Cross correlation between the monthly mean eastward velocity and river discharge into each bay (Fig. 8). Estimated 95% confidence level on the correlation coefficients are shown in dash lines

North Atlantic and the coast, ignoring small-scale local wind variations. Despite this wind imitation, the correlation coefficients are significant at over 99.8% confidence ( $R=0.25$ , 0.55 and 0.61, for CB, DB and NB, respectively; Table 1), meaning that the large-scale mean wind is responsible for about 6–37% of the monthly flow variability with more influence on the two northern bays.

Past studies focused on remote influence of the Atlantic Ocean and the Gulf Stream on coastal sea level (Ezer et al. 2013; Ezer 2015, 2023a; Dangendorf et al. 2021, 2023), but little research is done on remote influence on currents near bays – one exception is the study of Ezer and Updyke (2024) that shows potential links between surface currents

in the CB and the Atlantic Meridional Overturning Circulation (AMOC). The large-scale atmospheric pattern over the North Atlantic can be characterized by the North Atlantic Oscillation (NAO) index (Hurrell 1995), whereas positive phase indicates storm track farther north and more wet and stormy weather over the northeastern U.S., while negative phase indicates southern shift in the storm track, dryer weather and fewer storms over the same region. To evaluate the impact of NAO, it is compared with the surface velocity of the three bays (Fig. 12; Table 1). The monthly records were filtered by a 6-month Hanning Filter to remove high-frequency noise and focus on interannual to decadal NAO variability. The comparisons show statistically significant positive correlations (99–99.9% confidence) between NAO and the flow velocity – when NAO is positive/negative flow is generally stronger/weaker. There are however some exceptions, for example during 2018 when NAO was especially high, flow from CB was also high, but flows from DB and NB were lower than normal. Such variations are expected since wind can vary significantly with latitude. Two periods of more coherent flow peaks in the three bays that are consistent with the positive correlation are seen around May 2019 (NAO in a negative phase and all three bays show weak flow), and January 2020 (NAO in a positive phase and all three bays show larger flow, especially DB and NB). The wind pattern of these two periods from NCEP/NCAR reanalysis (Fig. 13) can explain the change in the observed flow. In May 2019 (negative NAO) wind pattern shifted southward (Fig. 13a), so that monthly mean wind speed in the study area was weak ( $\sim 0.5$ – $1.5$  m/s), while in January 2020 (positive NAO) stronger westerly winds ( $\sim 3.5$  m/s) may have caused the increased eastward flow seen in the data. The pattern in Fig. 13 is generally consistent with the NAO pattern described above – similar patterns are also seen in other months with significant anomalies.

It is useful to note that NAO pattern can affect temperatures, storm tracks and regional precipitation. However, the correlations between monthly NAO and monthly river run-offs into the bays were not statistically significant, so these correlations are not listed in Table 1.

## 4 Summary and conclusions

This research followed on the footsteps of recent studies of CB that found potential influence from Atlantic Ocean variability on observed sea level in the bay and on surface currents near the mouth of the bay (Ezer 2023a; Ezer and Updyke 2024). Here- we expanded the CB study by analyzing the surface currents obtained by high frequency radars near the mouths of three bays- CB, DB and NB. The goal was to find if statistically significant correlations exist between the flow variabilities of the three bays, and



**Fig. 10** Correlation between surface eastward current anomaly near the mouth of CB and local wind at 4 locations as a function of the angle between the wind and current direction. Positive angle means that the current direction is to the right of the wind. The inset shows the locations of the wind stations (one station, CBBT was relocated as indicated)

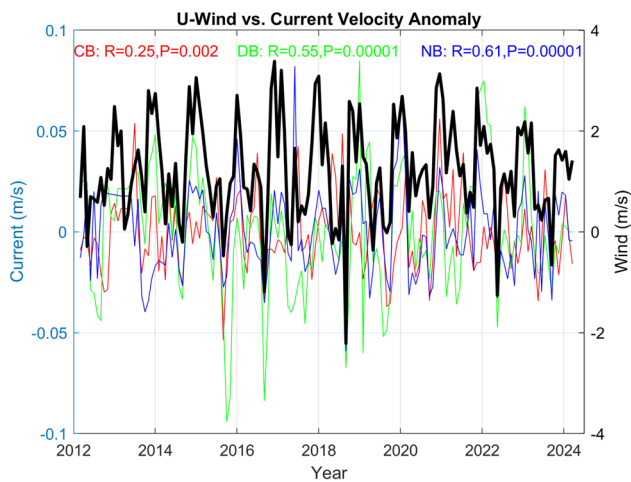
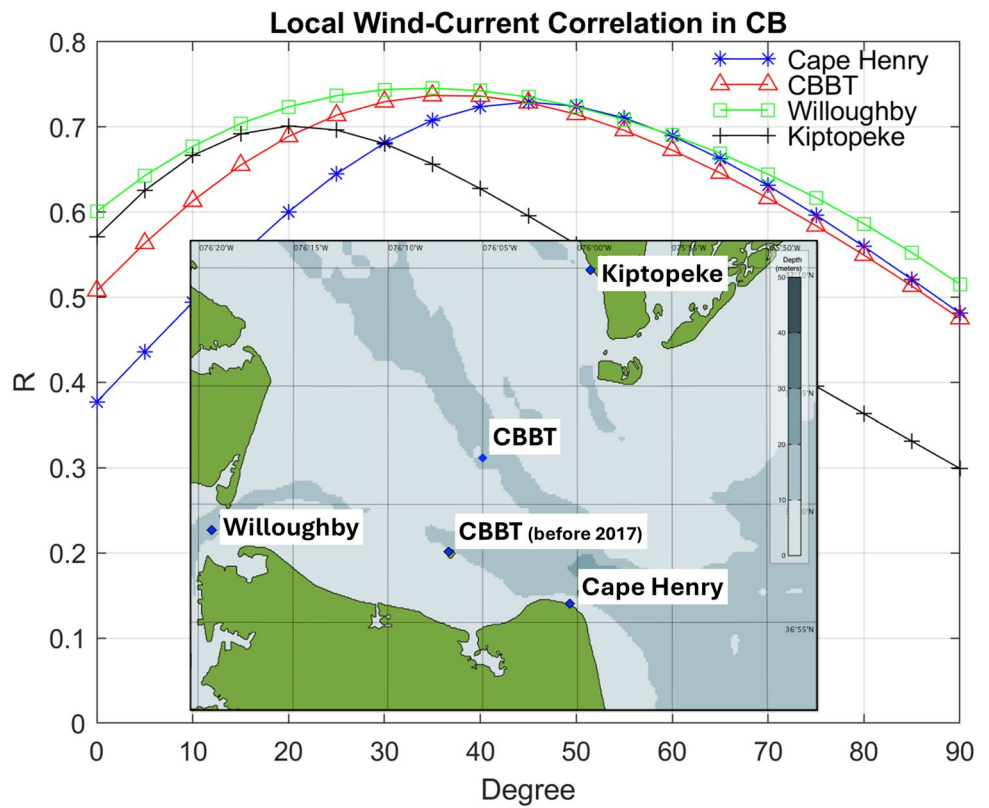


**Fig. 11** Monthly U-component of mean wind over the region from reanalysis data (heavy black line; y-axis on the right) versus the current velocity at the three bays (color lines; y-axis on the left). The correlations for the three bays are indicated

to investigate the sources of these correlations - are they driven by river discharges into the bays, local wind, or by remote influences on the currents from large-scale Atlantic Ocean variability?

The main findings can be summarized as follows.

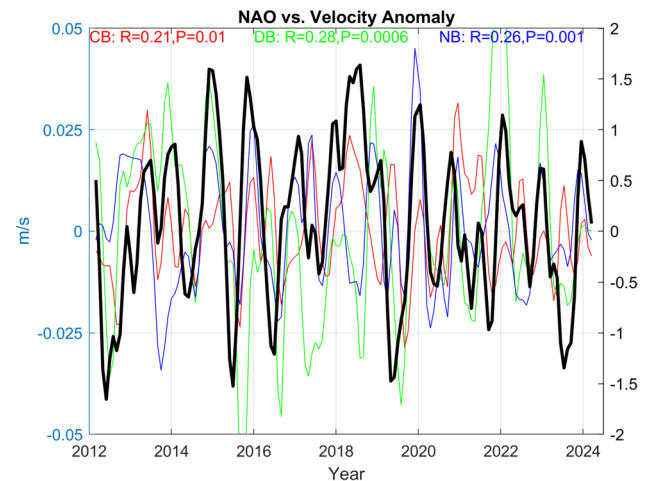


**Fig. 12** Monthly NAO index (black; heavy line, right axis) versus velocity anomaly in CB (red), DB (green) and NB (blue). High-frequency variability was smoothed with a 6-month Hanning Filter. Correlation coefficients are also listed

1. The patterns of surface flow near the mouth of the three bays have similarities in that a strong flow is seen near the southern side of the mouth where the plume of fresher waters turn to the right due to the Coriolis effect. The flow near the mouth of DB is somewhat different than the other bays, with southwestward flow along the

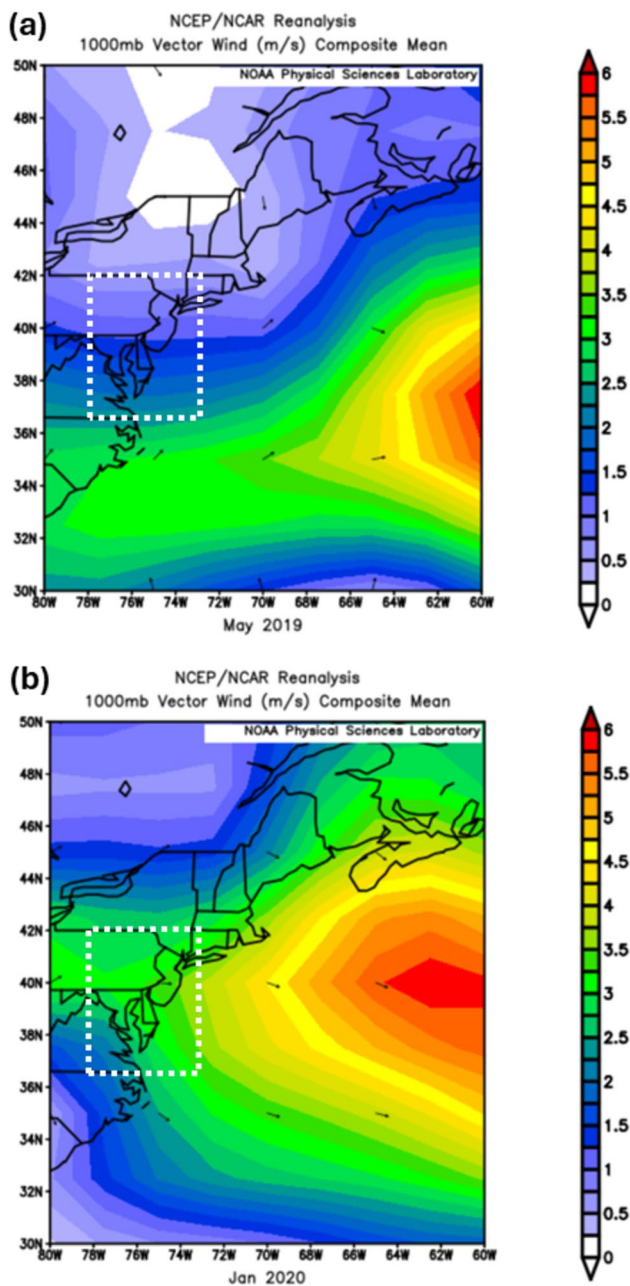


**Fig. 13** Monthly mean wind pattern from NCEP/NCAR Reanalysis (speed in color and direction in vectors) during **a** May 2019 when NAO was in a negative phase (monthly index of  $-1.62$ ) and **b** January 2020 when NAO was in a positive phase (monthly index of  $+1.34$ ). The study area is indicated by the dashed line

entrance to the bay before turning southeastward. This pattern was previously reported by other studies (see Fig. 9 in Muscarella et al. 2011) and is likely driven by the local winds and local topography. In particular, the deep and wide channel in DB may stir this flow. Unlike past studies, the focus here was not only on the local circulation patterns, but also on the long-term variability

using longer records than previous studies, and for the first time comparing three different bays.

2. There is a statistically significant, although relatively weak, correlation between the variability of the mean surface flow from the three bays, pointing to contribution from common forcing sources. Only about 10–15% of the variability can be explained by the common source, pointing to forcing that combines local factors unique for each bay as well as regional factors that affect the entire Mid-Atlantic Bight area.
3. A somewhat surprising result was the trend of eastward flow over time. Ezer and Updyke (2024) found significant upward trend in CB during the 2007–2016 period of their analysis that was linked with long-term increased precipitation and river discharges in the region (Rice et al. 2017). In this study for the 2012–2024 period there was no significant trend in the CB, while a significant upward trend of about 4 cm/s per decade was found in DB and NB. It seems that decadal and interannual variations are responsible for the change in trend in the CB. The increased streamflow into the CB before 2019 and decreased streamflow afterward (Fig. 6), are partly due to extreme winter snowstorms in 2018 and 2019 and unusually high river flows during these years. The result is a change in eastward flow trend in the CB from positive to negative around 2018–2019. The other two bays, which are fed by a single river each, do not have the large shift in river discharge and flow as seen in CB, and thus maintain a positive trend of increased outflow.
4. River discharge flow into each bay is significantly correlated with the observed flow near the mouth of the bay over seasonal and interannual time scales. However, only  $\sim 10\%$  of the monthly flow variability can be explained by the river discharge alone. However, for the seasonal cycle, correlation of river discharge and flow is higher, so up to  $\sim 40\%$  of the seasonal flow variability can be explained by the seasonal river discharge. In the CB cross correlation indicates a delay lag of 2–3 months in the response of surface currents to the seasonal river discharge. No clear lag was found in the other bays due to large interannual variability and other factors affecting the flow.
5. An interesting finding was that extreme peaks in surface currents, that are seen simultaneously in all bays at the same month, are often related to extreme weather events. During months in the fall when hurricanes were observed in the western North Atlantic, anomalous large flows into the bays were recorded, while during winter storms anomalous large flows out of the bays were recorded. The impact of hurricanes – i.e., the increased flows toward bays – is consistent with their impact on raising coastal sea level during and after hurricanes

(Ezer et al. 2017; Ezer 2019, 2020b; Park et al. 2022, 2024).

6. The NAO index was found to be significantly correlated with the flow near the mouth of the bays, but only about 5–10% of the variability is explained by the NAO. The positive correlation between NAO and the flows suggests that during positive phases of the NAO there is increased flow from the bays. The wind pattern over the area during positive NAO indeed shows stronger westerly winds (eastward) that is consistent with increased flow from the bays toward the open ocean. During negative NAO phases the storm track moves southward of the study area, the westerly (eastward) winds are weaker, and eastward flows are relatively weaker. This pattern is consistent with studies that show increased sea level and flooding during periods of very negative NAO (Ezer 2015; Goddard et al. 2015). As expected from past studies, local wind-driven Ekman flow is significant even on monthly basis, but about 50% of the variability is still contributed by other factors. It is interesting to note that other coastal regions also show that in addition to local winds and river runoffs, significant part of the variability is attributed to large scale remote influence. For example, large scale atmospheric pressure patterns over the Pacific Ocean can affect the dynamics in the San Francisco Bay (Wang et al. 1997), and the Atlantic Multidecadal Oscillation (AMO) and the Pacific Decadal Oscillation (PDO) can affect variations in temperatures and ice coverage over the Great Lakes (Wang et al. 2018). These decadal and multidecadal patterns may affect temperatures and precipitation along the U.S. East Coast, including the bays, but the 12-years record of surface currents analyzed here is too short for detecting decadal and multidecadal variabilities.

In summary, the study of surface currents from high-frequency radars shows a complex pattern of velocities near the mouth of three major U.S. East Coast bays. While recognizing that the surface flow may not fully represent the total transport in and out of the bay, to our knowledge, this is the first study that compares these three bays using this type of data for relatively long period (12 years). The surface currents seem to be driven by multiple sources, local and remote, that include river discharges, tropical storms and hurricanes, winter storms, and changing wind patterns over the Atlantic Ocean associated with large-scale climate variability; each of these drivers contributes a portion of the observed variability, so there is no one dominant factor. While the three bays are separated by some 400 km, have different topographies and sizes, and have input from different watersheds and different rivers, there are similarities in their flow variability that suggest common drivers that may affect a long stretch of the U.S.

East Coast and especially the Mid-Atlantic Bight where the bays are situated. The study is important for better understanding coastal dynamics and potential impacts of climate change on the highly populated coastal communities and cities along the U.S. East Coast.

**Acknowledgements** The research is supported by collaboration with ODU's Institute for Coastal Adaptation and Resilience (ICAR) and the Center for Coastal Physical Oceanography (CCPO). The CODAR maintenance work of T. Updyke is funded by NOAA's Mid-Atlantic Regional Association Coastal Ocean Observing System (MARACOOS; Award #NA21NOS0120096).

**Author contributions** T.E. and T.U. analyze the data, made figures, wrote and edit the text. All authors reviewed the manuscript.

**Funding** NOAA funding for 2<sup>nd</sup> author is indicated in the Acknowledgements.

**Data availability** Links to all data sources are included in the manuscript.

## Declarations

**Competing interests** The authors declare no competing interests.

**Open Access** This article is licensed under a Creative Commons Attribution 4.0 International License, which permits use, sharing, adaptation, distribution and reproduction in any medium or format, as long as you give appropriate credit to the original author(s) and the source, provide a link to the Creative Commons licence, and indicate if changes were made. The images or other third party material in this article are included in the article's Creative Commons licence, unless indicated otherwise in a credit line to the material. If material is not included in the article's Creative Commons licence and your intended use is not permitted by statutory regulation or exceeds the permitted use, you will need to obtain permission directly from the copyright holder. To view a copy of this licence, visit <http://creativecommons.org/licenses/by/4.0/>.

## References

- Atkinson LP, Garner T, Blanco J, Paternostro C, Burke P (2009) HFR surface currents observing system in lower Chesapeake Bay and Virginia coast. OCEANS 2009, Biloxi, MS, USA, 26–29 October 2009, pp 1–6. <https://doi.org/10.23919/OCEANS.2009.5422254>
- Blumberg AF, Ali Khan L, St. John JP (1999) Three-dimensional hydrodynamic model of New York Harbor region. J Hydr Eng 125(8). [https://doi.org/10.1061/\(ASCE\)0733-9429\(1999\)125:8\(799\)](https://doi.org/10.1061/(ASCE)0733-9429(1999)125:8(799))
- Chen G, Wang WC, Cheng CT, Hsu HH (2021) Extreme snow events along the coast of the northeast United States: potential changes due to global warming. J Clim 34(6):2337–2353. <https://doi.org/10.1175/JCLI-D-20-0197.1>
- Dangendorf S, Frederikse T, Chafik L, Klinck J, Ezer T, Hamlington B (2021) Data-driven reconstruction reveals large-scale ocean circulation control on coastal sea level. Nat Clim Change 11:514–520. <https://doi.org/10.1038/s41558-021-01046-1>
- Dangendorf S, Hendricks N, Sun Q, Klinck J, Ezer T, Frederikse T, Calafat FM, Wahl T, Törnqvist TE (2023) Acceleration of U.S. Southeast and Gulf coast sea-level rise amplified by internal



- climate variability. *Nat Commun* 14:1935. <https://doi.org/10.1038/s41467-023-37649-9>
- Domingues R, Goni G, Baringer M, Volkov D (2018) What caused the accelerated sea level changes along the U.S. East Coast during 2010–2015? *Geophys Res Lett* 45(24):13367–13376. <https://doi.org/10.1029/2018GL081183>
- Ezer T (2015) Detecting changes in the transport of the Gulf Stream and the Atlantic overturning circulation from coastal sea level data: the extreme decline in 2009–2010 and estimated variations for 1935–2012. *Glob Planet Change* 129:23–36. <https://doi.org/10.1016/j.gloplacha.2015.03.002>
- Ezer T (2019) Hurricanes and the gulf stream: a double whammy impact on coastal flooding. *CCPO Circulation*, 24(2). <http://www.ccpo.edu.edu/Circulation/2019/spring2019.pdf>
- Ezer T (2020a) Analysis of the changing patterns of seasonal flooding along the U.S. East Coast. *Ocean Dyn* 70(2):241–255. <https://doi.org/10.1007/s10236-019-01326-7>
- Ezer T (2020b) The long-term and far-reaching impact of hurricane dorian (2019) on the gulf stream and the coast. *J Mar Sys* 208. <https://doi.org/10.1016/j.jmarsys.2020.103370>
- Ezer T (2022) A demonstration of a simple methodology of flood prediction for a coastal city under threat of sea level rise: the case of Norfolk, VA, USA. *Earths Future* 10(9). <https://doi.org/10.1029/2022EF002786>
- Ezer T (2023a) Sea level acceleration and variability in the Chesapeake Bay: past trends, future projections, and spatial variations within the. *Bay Ocean Dyn* 73(1):23–34. <https://doi.org/10.1007/s10236-022-01536-6>
- Ezer T (2023b) Evaluation of the applicability of the Ekman theory for wind-driven ocean currents: a comparison with the Mellor-Yamada turbulent model. *Ocean Dyn* 73. <https://doi.org/10.1007/s10236-023-01570-y>
- Ezer T, Atkinson LP (2014) Accelerated flooding along the U.S. East Coast: on the impact of sea-level rise, tides, storms, the gulf stream, and the North Atlantic Oscillations. *Earths Future* 2(8):362–382. <https://doi.org/10.1002/2014EF000252>
- Ezer T, Atkinson LP (2017) On the predictability of high water level along the U.S. East Coast: can the Florida current measurement be an indicator for flooding caused by remote forcing? *Ocean Dyn* 67(6):751–766. <https://doi.org/10.1007/s10236-017-1057-0>
- Ezer T, Atkinson LP, Corlett WB, Blanco JL (2013) Gulf Stream's induced sea level rise and variability along the U.S. mid-atlantic coast. *J Geophys Res* 118(2):685–697. <https://doi.org/10.1002/jgrc.20091>
- Ezer T, Atkinson LP, Tuleya R (2017) Observations and operational model simulations reveal the impact of Hurricane Matthew (2016) on the Gulf Stream and coastal sea level. *Dyn Atmos Oceans* 80:124–138. <https://doi.org/10.1016/j.dynatmoce.2017.10.006>
- Ezer T, Corlett WB (2012) Is sea level rise accelerating in the Chesapeake Bay? A demonstration of a novel new approach for analyzing sea level data. *Geophys Res Lett* 39(19):L19605. <https://doi.org/10.1029/2012GL053435>
- Ezer T, Henderson-Griswold S, Updyke T (2022) Dynamic observations in the Hampton Roads region: how surface currents at the mouth of Chesapeake Bay may be linked with winds, water level, river discharge and remote forcing from the Gulf Stream. *Oceans 2022. IEEE Xplore*. <https://doi.org/10.1109/OCEANS47191.2022.9977092>
- Ezer T, Updyke T (2024) On the links between sea level and temperature variations in the Chesapeake Bay and the Atlantic Meridional Overturning Circulation (AMOC). <https://doi.org/10.1007/s10236-024-01605-y>. *Ocean Dyn* 74
- Galperin B, Mellor GL (1990) A time-dependent, three-dimensional model of the Delaware Bay and River system. Part 2: three-dimensional flow fields and residual circulation. *Est Coast Shelf Sci* 31(3):255–281. [https://doi.org/10.1016/0272-7714\(90\)90104-Y](https://doi.org/10.1016/0272-7714(90)90104-Y)
- Garvine RW (1991) Subtidal frequency estuary-shelf interaction: observations near Delaware Bay. *J Geophys Res Oceans* 96(C4):7049–7064. <https://doi.org/10.1029/91JC00079>
- Goddard PB, Yin J, Griffies SM, Zhang S (2015) An extreme event of sea-level rise along the Northeast coast of North America in 2009–2010. *Nat Commun*. <https://doi.org/10.1038/ncomms7346>
- Gopalakrishnan G, Blumberg AF (2012) Assimilation of HF radar-derived surface currents on tidal-timescales. *J Oper Oceanogr* 5(1):75–87. <https://doi.org/10.1080/1755876X.2012.11020133>
- Hurrell JW (1995) Decadal trends in the North Atlantic oscillation: regional temperatures and precipitation. *Science* 269:676–679. <https://doi.org/10.1126/science.269.5224.676>
- Li Y, Feng H, Zhang H, Sun J, Yuan D, Guo L, Nie J, Du J (2019) Hydrodynamics and water circulation in the New York/New Jersey Harbor: a study from the perspective of water age. *J Mar Sys* 199. <https://doi.org/10.1016/j.jmarsys.2019.103219>
- Little CM, Hu A, Hughes CW, McCarthy GD, Piecuch CG, Ponte RM, Thomas MD (2019) The relationship between U.S. East Coast Sea Level and the Atlantic Meridional overturning circulation: a review. *J Geophys Res* 124(9):6435–6458. <https://doi.org/10.1029/2019JC015152>
- Moat BI, Smeed DA, Rayner D, Johns WE, Smith R, Volkov D, Baringer MO, Collins J (2023) Atlantic meridional overturning circulation observed by the RAPID-MOCHA-WBTS (RAPID-Meridional overturning circulation and heatflux array-western Boundary Time Series) array at 26 N from 2004 to 2022 (v2022.1). *Br Oceanogr Data Centre - Nat Environ Res Council UK*. <https://doi.org/10.5285/04c79ece-3186-349a-e063-6c86abc0158c>
- Muscarella PA, Barton NP, Lipphardt BL Jr, Veron DE, Wong KC, Kirwan AD Jr. (2011) Surface currents and winds at the Delaware Bay mouth. *Cont Shelf Res* 31(12):1282–1293. <https://doi.org/10.1016/j.csr.2011.05.003>
- Park K, Di Lorenzo E, Zhang YJ, Wang H, Ezer T, Ye F (2024) Delayed coastal inundation caused by ocean dynamics post-hurricane Matthew. *NPJ Clim Atmos Sci* 7:5. <https://doi.org/10.1038/s41612-023-00549-2>
- Park K, Federico I, Di Lorenzo E, Ezer T, Cobb KM, Pinardi N, Coppi G (2022) The contribution of hurricane remote ocean forcing to storm surge along the Southeastern U.S. coast. *Coastal Eng* 173:104098. <https://doi.org/10.1016/j.coastaleng.2022.104098>
- Piecuch CG, Dangendorf S, Gawarkiewicz GG, Little CM, Ponte RM, Yang J (2019) How is New England coastal sea level related to the Atlantic meridional overturning circulation at 26°N? *Geophys Res Lett* 46. <https://doi.org/10.1029/2019GL083073>
- Rice KC, Moyer DL, Mills AL (2017) Riverine discharges to Chesapeake Bay: analysis of long-term (1927–2014) records and implications for future flows in the Chesapeake Bay Basin. *J Env Mng* 204(1):246–254. <https://doi.org/10.1016/j.jenvman.2017.08.057>
- Sharp JH, Cifuentes LA, Coffin RB, Pennock JR, Wong KC (1986) The influence of river variability on the circulation, chemistry, and microbiology of the Delaware Estuary. *Estuaries* 9:261–269. <https://doi.org/10.2307/1352098>
- Smeed DA, McCarthy GD, Cunningham SA, Frajka-Williams E, Rayner D, Johns WE, Meinen CS, Baringer MO, Moat B, Ducez A, Bryden HL (2014) Observed decline of the Atlantic meridional overturning circulation 2004–2012. *Ocean Sci* 10:29–38. <https://doi.org/10.5194/os-10-29-2014>
- Sweet W, Park J (2014) From the extreme to the mean: acceleration and tipping points of coastal inundation from sea level rise. *Earths Future* 2(12):579–600. <https://doi.org/10.1002/2014EF000272>
- Valle-Levinson A (2010) Definition and classification of estuaries. Contemporary issues in Estuarine Physics 1–11. Valle-Levinson (Ed), Cambridge Univ. Press, Cambridge, UK. <https://doi.org/10.1017/CBO9780511676567.002>



- Valle-Levinson A, Boicourt WC, Roman MR (2003) On the linkages among density, flow, and bathymetry gradients at the entrance to the Chesapeake Bay. *Estuaries* 26:1437–1449. <https://doi.org/10.1007/BF02803652>
- Valle-Levinson A, Dutton A, Martin JB (2017) Spatial and temporal variability of sea level rise hot spots over the eastern United States. *Geophys Res Lett* 44(15):7876–7882. <https://doi.org/10.1002/2017GL073926>
- Valle-Levinson A, Li C, Royer TC, Atkinson LP (1998) Flow patterns at the Chesapeake Bay entrance. *Cont Shelf Res* 18(10):1157–1177. [https://doi.org/10.1016/S0278-4343\(98\)00036-3](https://doi.org/10.1016/S0278-4343(98)00036-3)
- Volkov D, Zhang K, Johns W, Willis J, Hobbs W, Goes M, Zhang H, Menemenlis D (2023) Atlantic meridional overturning circulation increases flood risk along the United States southeast coast. *Nat Comm* 14:5095. <https://doi.org/10.1038/s41467-023-40848-z>
- Volkov DL, Lee S-K, Domingues R, Zhang H, Goes M (2019) Interannual sea level variability along the southeastern seaboard of the United States in relation to the gyre-scale heat divergence in the North Atlantic. *Geophys Res Lett*. <https://doi.org/10.1029/2019GL083596>
- Wang J, Cheng RT, Smith PC (1997) Seasonal sea-level variations in San Francisco Bay in response to atmospheric forcing, 1980. *Estuar Coastal Shelf Sci* 45(1):39–52. <https://doi.org/10.1006/ecss.1996.0162>
- Wang J, Kessler J, Bai X, Clites A, Lofgren B, Assuncao A, Bratton J, Chu P, Leshkevich G (2018) Decadal variability of Great Lakes ice cover in response to AMO and PDO, 1963–2017. *J Clim* 31(18):7249–7268. <https://doi.org/10.1175/JCLI-D-17-0283.1>
- Wong K-C, Garvine RW (1984) Observations of wind-induced, subtidal variability in the Delaware estuary. *J Geophys Res Oceans* 89(C6):10589–10597. <https://doi.org/10.1029/JC089iC06p10589>

**Publisher's note** Springer Nature remains neutral with regard to jurisdictional claims in published maps and institutional affiliations.